WPEDU-CPR(17) 18529

A Ross et al.

Non-Boussinesq turbulence studies for the scrape-off layer

Preprint of Paper to be submitted for publication in Proceeding of 16th International Workshop on Plasma Edge Theory in Fusion Devices (PET)

This work has been carried out within the framework of the EUROfusion Consortium and has received funding from the Euratom research and training programme 2014-2018 under grant agreement No 633053. The views and opinions expressed herein do not necessarily reflect those of the European Commission.

Article Type

Non-Boussinesq turbulence studies for the scrape-off layer

Alexander Ross,[1] Andreas Stegmeir,[1] and David Coster[1]

[1] *Max-Planck-Institut für Plasmaphysik, D-85748 Garching, Germany*

Correspondence: Email: Alexander.Ross@ipp.mpg.de

Summary

The drift-reduced global Braginskii system is implemented in GRILLIX, a plasma turbulence code able to treat diverted geometries, by using the flux-coordinate independent approach (FCI). We solve a 4-field model evolving the density, the electron temperature, the vorticity and parallel ion momentum. The difference between the system with the Boussinesq approximation (BS) and the full system (FS) is investigated. The Boussinesq approxiamtion is widely used since it reduces the numerical and computational complexity significantly. In order to understand the impact of the Boussinesq approximation a flux tube geometry is chosen as the computational domain. The conservation of energy and particles is derived and tested within the code, both in FS and BS. Moreover, we will discuss that the Boussinesq approximation has subtle effects on the energy theorem of the model, and a conserved energy-like quantity is only obtained if the Boussinesq approximation is applied in a consistent way. We will also present numerical and computational techniques in order to relax the Boussinesq approximation. The code is validated by the method of manufactured solutions, which yields the expected order of accuracy.

Keywords: Boussinesq-approximation, turbulence, Flux-coordinate independent (FCI), edge, method of manufactured solutions (MMS)

1 Inroduction

The understanding of turbulence in the scrape-off layer (SOL) is of major importance for future fusion devices. Turbulent transport of particles and heat out of the core plasma mainly affects the plasma confinement characteristics of the entire device [?freidberg] . Large amplitude effects like filaments and blobs may have a strong impact on the plasma-wall interaction. In the edge of a tokamak, where the plasma has a low temperature and high collisionality, a fluid model is appropriate. The Braginskii set of equations [?braginskii] is suitable for the description of the effects in the edge region, however it demands too heavy computational resources. Using the fact that plasma confinement

is mainly determined by low frequency dynamics, a drift reduced model can be used from the Braginskii system more suited for numerical treatment [?zeiler]. In addition the Boussinesq approximation is often employed, which reduces the numerical and computational complexity significantly. However, its use becomes questionable in the SOL where large fluctuations compared to the background may appear[?xu]. Consequently the relaxation of the Boussinesq approximation is an important part in a plasma turbulence code suitable for the edge region. Its impact on isolated blobs has been studied in [?bousblob]. Here we investigate the impact of the Boussinesq approximation on a turbulence simulation.

2 Physical model

The drift reduced Braginskii system is solved in a periodic slab geometry (e_x, e_y, e_z), where the poloidal coordinate is $y \in [y_{min}, y_{max}]$, the radial coordinate is given by $x \in [x_{min}, x_{max}]$ and the toroidal coordinate is $z \in [0, 2\pi]$. A constant magnetic field $\mathbf{B} = B_0 e_z$ is applied in the whole domain.

2.1 Equations

We employ the drift reduced Braginskii equations from [?zeiler], where we furthermore neglect electron inertia ($m_e/m_i \ll 1$) and the magnetic induction ($\beta_e \equiv 4\pi p_e/B^2 \ll 1$). Cold ions $T_i = 0$ are assumed, but the electron temperature T_e is kept in the governing model. Moreover, the polarization drift is neglected in the advective derivative. In the following all quantities are normalized according to $\hat{t} = \frac{c_s}{L_\parallel} t$, $\hat{x}_\perp = \frac{x_\perp}{\rho_s}$, $\hat{n} = \frac{n}{n_0}$, $\hat{\phi} = \frac{e\phi}{T_0}$, $\hat{\mathbf{B}} = \frac{\mathbf{B}}{B_0}$, $\hat{u}_\parallel = \frac{u_\parallel}{c_s}$, $\hat{j}_\parallel = \frac{j_\parallel}{c_s e n_0}$, $\hat{x}_\parallel = \frac{x_\parallel}{L_\parallel}$, $\hat{T}_e = \frac{T_e}{T_0}$. The normalized quantities are on the left side under hat, which will be dropped in the following for clarity and conciseness. The perpendicular direction is normalized with the ion sound radius $\rho_s = c\sqrt{T_e M_i}/eB_0$. The coordinates are given in terms of some characteristic length scale $L_\parallel$. This fixes the dimensionless parameter $\delta = \rho_s/L_\parallel$. Time is measured in terms of $L_\parallel/c_s$ with the sound speed $c_s = \sqrt{T_e e/m_i}$. The density, the magnetic field and the electron temperature are normalized to some reference values n_0, B_0, T_0, respectively. Under the drift reduction the perpendicular velocities of the electrons and ions can be written as $v_{e\perp} = v_{E\times B} + v_d$ and $v_{i\perp} = v_{E\times B} + v_{pol}$ where the $E \times B$-drift $v_{E\times B}$, the diamagnetic drift v_d and the polarization drift u_p are defined respectively as $v_{E\times B} = e_z \times \nabla\phi$, $v_d = -e_z \times \nabla p_e/n$ and $u_p = \delta e_z \times \frac{d_i}{dt} v_{E\times B}$. The resulting system of equations in normalized units can be written as

$$\frac{\partial}{\partial t}n + \delta^{-1}\left[\phi, n\right] = nC(\phi) - C(p_e) - \nabla\cdot\Big[nv_{\parallel e}\mathbf{b}\Big] + D(n) + S_n, \quad (1)$$

$$\frac{\partial}{\partial t}u_\parallel + \delta^{-1}\Big[\phi, u_\parallel\Big] + u_\parallel\nabla_\parallel u_\parallel = -\frac{1}{n}\nabla_\parallel p_e + D(u_\parallel), \quad (2)$$

$$\frac{\partial}{\partial t}T_e + \delta^{-1}\left[\phi, T_e\right] = \frac{4}{3}\big[\frac{T_e^2}{n}C(n) + \frac{7}{2}T_eC(T_e) - T_eC(\phi)\big] + \frac{2}{3}\frac{0.71}{n}T_e\nabla\cdot\frac{j_\parallel}{e}\mathbf{b} - \frac{2}{3}T_e\nabla_\parallel v_{\parallel e} - v_{\parallel e}\nabla_\parallel T_e + D(T_e) + S_t, \quad (3)$$

$$\nabla\cdot\Big[n\frac{\partial}{\partial t}\nabla_\perp\phi\Big] + \delta^{-1}\nabla\cdot n\left[\phi, \nabla_\perp\phi\right] + \nabla\cdot nu_\parallel\nabla_\parallel\nabla_\perp\phi = -C(p_e) + \nabla\cdot\Big[\mathbf{b}j_\parallel\Big] + D(\omega), \quad (4)$$

$$\frac{j_\parallel}{\sigma_\parallel} = -\nabla_\parallel\phi + \frac{T_e}{en}\nabla_\parallel n + 1.71\nabla_\parallel T_e \quad (5)$$

where the dimensionless conductivity $\sigma_\parallel = \frac{c_s}{R_0}\frac{m_i}{m_e}\frac{1}{0.51\nu_e}$ and the generalized vorticity is given by $\omega^{FS} = \nabla\cdot n\nabla_\perp\phi$. The operator $C(f) = -2\frac{\partial}{\partial y}f$ models the curvature of the magnetic field. The plasma exhaust from the core is modeled with the gaussian source terms S_n and S_t. We add diffusion terms in perpendicular and parallel direction $D(f) = \nabla\cdot\big[\nu_f\nabla_\perp f\big] + \nabla\cdot\big[\mu_f\nabla_\parallel f\big]$ respectively. The $E\times B$-advection is written as an Arakawa bracket $[\phi, f] = \partial_x\phi\partial_y f - \partial_y\phi\partial_x f$ [?arakawa].

2.2 Energy theorem

The total energy theorem of the system consists of the perpendicular kinetic energy $E_\perp = \frac{1}{2}n\mathbf{v}_e^2$, the ion parallel kinetic energy $E_\parallel = \frac{1}{2}n\mathbf{v}_{\parallel i}^2$ and the thermal energy $E_T = \frac{3}{2}p_e$. Summing the energies contained in the system yields,

$$\frac{\partial}{\partial t}\int dV[E_\perp + E_\parallel + E_T] = \int dV[-\frac{j_\parallel^2}{\sigma} + C_{SD} + C_p]. \quad (6)$$

where the surface have no contribution with the proper choice of boundary conditions discussed in the next section. The first term on the right side is the ohmic heating acting as an energy sink. This term appears due to the neglect of ohmic heating in the temperature equation as was also shown in [?zeiler]. The second part

$$C_{SD} = \frac{1}{2}M_iv_e^2(D(n) - D(\omega^{FS})_\perp + S_n) + \frac{1}{2}M_i\mathbf{v}_{\parallel i}^2(D(n) - D(\omega^{FS})_\perp + S_n) + \frac{3}{2}T_e(D(n) + S_n) + \frac{3}{2}n(D(T) + S_T) - \phi D(\omega^{FS}) + n\mathbf{v}_{\parallel i}D(u_\parallel) - \frac{S_n\mathbf{u}_\parallel^2}{2}$$

are terms coming from the sources and diffusion. The last correction term $C_p = -\frac{1}{2}n\mathbf{v}_{pol}\nabla\cdot(\mathbf{v}_{\parallel i}^2 + \mathbf{v}_e^2))$ appears in the energy equation due to the neglect of the polarization current in the advective derivative and is expected to be small. The energy theorem serves as a diagnostic and will be checked in section 4.

2.3 Boussinesq approximation

The Boussinesq approximation is widely used in the plasma turbulence community [?gbs, ?hermes, ?tokam, ?grillix4]. The main point of it is the assumption that the fluctuations of the density are very small compared to the background,

such that one neglects the spatial and temporal dependence of the density ($n(x,y,z,t) \to n_0 = 1$) in the vorticity equation leading to a simplification. One form of the Boussinesq approximation often used is $\nabla\cdot[n\frac{d}{dt}\nabla_\perp\phi] \to n_0\frac{d}{dt}\nabla^2_\perp\phi$ giving the left side of Eq. (4):

$$\frac{n_0}{B^2}\left[\frac{\partial}{\partial t}\nabla^2_\perp\phi\right] + \delta^{-1}\frac{n_0}{B^3}\left[\phi,\nabla^2_\perp\phi\right] + \frac{n_0}{B}u_\parallel\nabla_\parallel\nabla^2_\perp\phi, \tag{7}$$

where the Boussinesq vorticity is $\omega^{BS} = \nabla^2_\perp\phi$. No assumptions about the density fluctuations are made in the rest of the system. Of course this is a strong approximation, especially in the scrape-off layer where large amplitude fluctuations can occur. The main argument for the Boussinesq approximation is the simpler solution of the vorticity equation. There is no physical justification for it, if the main interest is the study of turbulence or large amplitude filaments in the scrape-off layer. One can construct an energy like quantity for the perpendicular kinetic energy $E^{BS}_\perp = \frac{1}{2}n_0\mathbf{v_e}$ in the Boussinesq approximation giving the modified energy theorem,

$$\frac{\partial}{\partial t}\int dV[E^{BS}_\perp + E_\parallel + E_T] = \int dV[-\frac{j^2_\parallel}{\sigma} + C_{SD} + C_p + C_{BS}], \tag{8}$$

The additional terms $C_{BS} = [\phi\mathbf{v}_e + \phi\mathbf{u}_\parallel\mathbf{b}]\cdot\nabla\omega^{BS}$ have no counterparts in the other energy equations, meaning that in the Boussinesq approximation the energy is not conserved anymore. In order to preserve the energy one has to neglect the parallel advetion of ω^{BS} and write $\phi\mathbf{v}_e\nabla\omega^{BS} = \nabla\cdot[\phi\omega^{BS}\mathbf{v}_e] - \omega^{BS}\phi\nabla\cdot\mathbf{v}_e$. Neglecting the divergence of $\mathbf{v}_e$ leads to a total divergence and a conserved energy. Consequently the Boussinesq approximation is much more than just neglecting spatial and temporal dependence of the density in the vorticity equation as it breaks the conservation properties $\nabla\cdot j = 0$ of the entire system. It requires two more strong assumptions that are not acceptable in general in the edge region and realistic geometries. Nevertheless one gets a consistent delta-f energy, which has to be conserved when applying the Boussinesq approximation. A conservative form of the Boussinesq approximation is shown in [?hermes, ?simankov]

2.4 Numerical implementation

The physical model is implemented in GRILLIX, which in general can treat complex geometries with die FCI approach [?grillix1, ?grillix2, ?grillix3]. Here we want to test and verify the global model with electron temperature staying in a slab geometry. In the poloidal planes we have a Cartesian grid such that standard finite differences can be used. For timestepping the Karniadakis scheme was employed [?bdf3]. Special attention is required in FS when discretizing the operators $\nabla\cdot(n\,[\phi,\nabla_\perp\phi])$ and $\nabla\cdot(nu_\parallel\nabla_\parallel\nabla_\perp\phi)$, which is realized on staggered grids, see Figure 1. For example in the operator $\nabla\cdot n\,[\phi,\nabla_\perp\phi]$ the perpendicular gradient maps ϕ to the staggered grid $\nabla_x\phi^{i\pm\frac{1}{2},j} = \pm\frac{\phi_{i+1,j}-\phi_{i,j}}{h}$

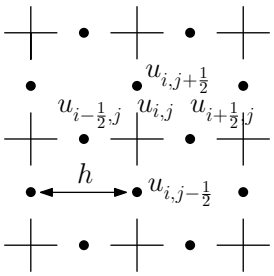

Figure 1: Quantity u is mapped to the staggered grid.

and $\nabla_y \phi^{i,j\pm\frac{1}{2}} = \pm\frac{\phi_{i,j+1}-\phi_{i,j}}{h}$. In order to evaluate the product between the density and the Arakawa bracket on the staggered grid, the denstiy and potential need to be mapped to the perpendicular staggered grid. The divergence maps the quantity back to the full grid. This procedure is required in order to get a consistent scheme for the $E\times B$-advection meaning that one receives the standard Arakawa bracket $[\phi, \nabla_\perp^2 \phi]$ when setting the density $n = n_0$. Otherwise the stencil skips neighboring grid points (checker-boarding). The numerical implementation of both operators is tested within the method of manufactured solution in the next section.

3 Verification by the method of manufactured solutions (MMS)

The implementation of the physical model in GRILLIX has been verified with the method of manufactured solutions [?mms], which is a standard procedure in the community [?mms2, ?mms3]. Our testing functions are given by

$$f(x,y,\rho,t) = [c_1 cos(k_1^\rho \rho) + s_1 sin(k_2^\rho \rho)] \cdot [c + sin(\psi + t\omega)] \cdot [e_1 e^{-ex\cdot\bar{x}} + c_2 cos(k_1^x \bar{x}) + s_2 sin(k_2^x \bar{x}] \cdot [c_3 cos(k_1^y \bar{y}) + s_3 sin(k_2^y \bar{y})]$$

with $\bar{x} = \frac{2\pi(x-x_{min})}{(x_{max}-x_{min})}, \bar{y} = \frac{2\pi(y-y_{min})}{(y_{max}-y_{min})}$ and arbitrary parameters $c_1, k_1^\rho, s_1, k_2^\rho, c, \psi, \omega, e_1, ex, c_2, s_2, k_1^x, k_2^x, c_3, s_3, k_1^y, k_2^y$ within the interval [0,2] for the density, the parallel momentum, the vorticity and the temperature. All parts of FS

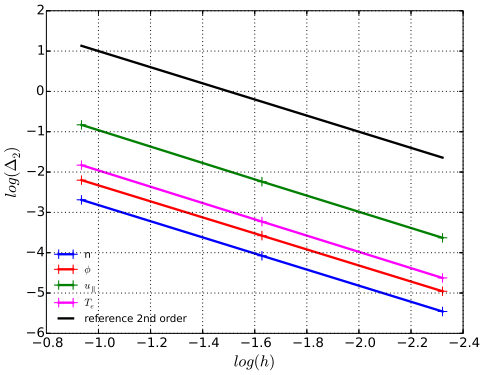

Figure 2: L2-Norm Δ_2 of the numerical error for the complete model. Second order accuracy of the implementation is confirmed.

were tested separatly. Here only the result for the complete model is presented without the sources S_n and S_t with

the parameters in the range of a typical turbulence simulation with $\sigma_{\parallel} = 2.5$, $\delta^{-1} = 580$, $\nu_{n,u,\omega,t} = 50$, $\mu_{n,u,\omega,t} = 0.1$. The domain ranges from $x_{min} = 0$ to $x_{max} = 64$ and $y_{min} = 0$ to $y_{max} = 64$. The resolution in the parallel direction of $\Delta\rho = \frac{2\pi}{16}/2^i$ and in the radial direction of $h = 4.0/2^i$ where $i = 0, 1, 2$ is covered. As shown in Figure 2 the numerical error in the L2-norm $\Delta_2 = |u_{num} - u_{ana}|_2/|u_{ana}|_2$ decreases with second order in the grid spacing as expected. Consequently the model was implemented correctly.

4 Turbulence simulations

In this section a turbulence simulation is performed for both the BS and FS. The parameters are given by $\sigma_0 = 1.5$, $\nu_{n,u,t,\phi} = 10$, $\mu_{n,u,t,\phi} = 10^{-2}$, $\delta^{-1} = 580$, $h = 0.5$, $\delta z = 2\pi/32$, $\rho_s = 1.0$, $x_{max} = 64$, $y_{max} = 64$. Density and electron temperature sources are modeled with the function $S(f) = c_{src}(f_{target} - < f >_{zonal})$, where c_{src} is a constant rate and f_{target} is the target value of the quantity. The volume averaged density and electron temperature, particle conservation and the energy theorem from Eq. (5) are shown in Figure 3. The energy is conserved up to the

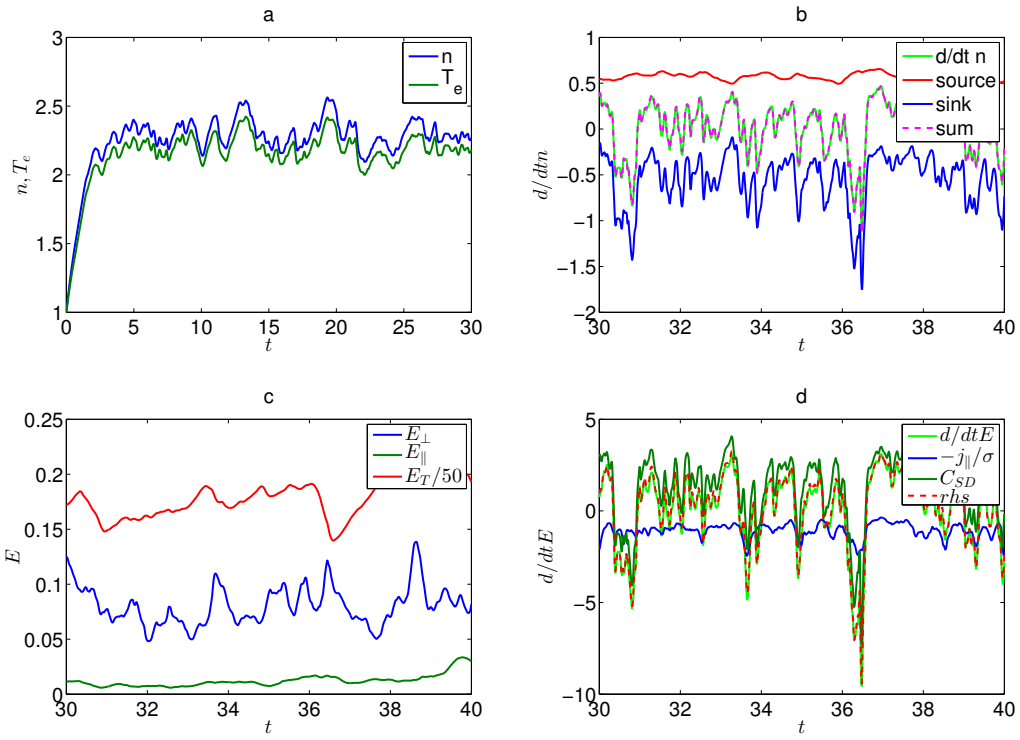

Figure 3: a) zonal average of n and T_e, both quantities are saturated. b) particle conservation. c) Kinetic and thermal energies of the system, thermal energy E_T is scaled by a factor of 50. d) Energy theorem shows good energy conservation.

correction terms coming from the ohmic heating, sources and diffusion. The correction term C_p was not included in

the diagnostics suggesting that these terms are indeed very small and can be neglected. The same result holds also for BS including the additional correction terms, see Eq. (7). In Figure 4 the profiles $< n >_{y,z,t}$ and $< T_e >_{y,z,t}$, the fluctuation level $\hat{f} = \sqrt{< \frac{f^2 - <f>^2}{<f>^2} >_{y,z,t}}$, convective and diffusive transport of particles $\Gamma_n = \Gamma_n^C + \Gamma_n^D = < nv_{E\times B} >_{y,z,t} + < D\partial_x n >_{y,z,t}$ and thermal energy $\Gamma_p = \Gamma_p^C + \Gamma_p^D = \frac{3}{2} < p_e v_{E\times B} >_{y,z,t} + \frac{3}{2} n < D(T_e) >_{y,z,t} + \frac{3}{2} T_e < D(n) >_{y,z,t}$ are shown for BS and FS. Here $< ... >_{y,z,t}$ indicates the poloidal, toroidal and time average, respectively. The biggest difference is the fluctuation level. There is a slight difference in the profile for both the density and

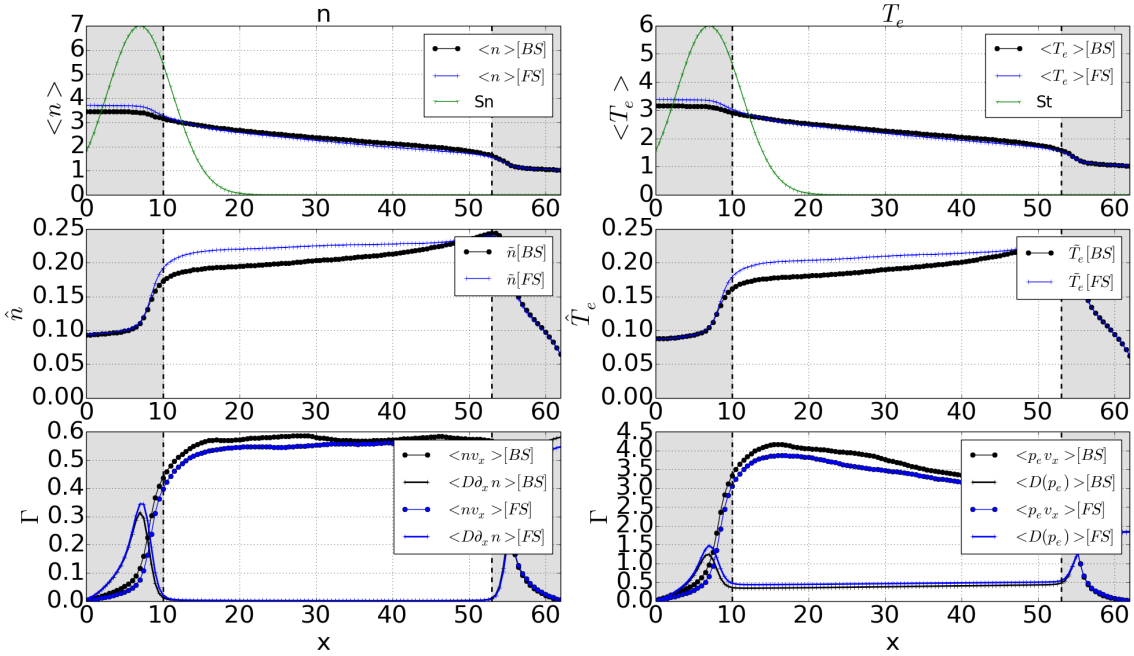

Figure 4: Comparison between BS (black) and FS (blue) for the profiles, the energy and particle transport and fluctuation levels.

temperature. Consequently the particle transport is higher in BS. The same holds for the energy transport. From a qualitative point of view there is no big impact of the Boussinesq approximation on turbulence dynamics at least for the chosen parameters and geometry. This result might change for steaper gradients in the density. Strong convective particle transport indicates that transport is dominated by turbulence in the source free region. The sloping convective transport of thermal energy arises due to the neglec of ohmic heating in the temperature equation as it acts as an energy transfer term.

5 Conclusion

Our code GRILLIX was extended to a full 4-field model without the Boussinesq approximation. It has been shown with the method of manufactured solutions that the model was implemented correctly. Furthermore the code conserves the energy and particles of the entire system. Saturated turbulence simulations have shown no big impact of the Boussinesq approximation on the dynamics. Another investigations with steaper density gradients and general geometry are needful and might change this result.

6 Outlook

The simulations in this work have been performed in a periodic slab geometry in order to relax on the Boussinesq approximation and understand the impact of it. The implementation of parallel boundaries is the next step for this geometry and has been already started. The final goal is the usage of the full capability of GRILLIX meaning that performing similar turbulence simulations in a realistic diverted geometry with X-point which was done in the Boussinesq approximation in [?grillix4].

Acknowledgments

This work has been carried out within the framework of the EUROfusion Consortium and has received funding from the Euratom research and training programme 2014-2018 under grant agreement No 633053. The views and opinions expressed herein do not necessarily reflect those of the European Commission.

References

[1] Jeffrey Freidberg, *Plasma Physics and Fusion Energy*, Cambridge University Press **2007**.

[2] Braginskii S I, *Review of Plasma Physics* **1965**, *1*.

[3] Zeiler A, Drake J F, Rogers B, *Phys. Plasmas* **1997**, *4(2134)*.

[4] Xu Y.H, Jachmich S, Weynants R.R, Weynants R.R, TEXTOR team, *Plasma Phys. Control Fusion* **2005**, *47*.

[5] Arakawa A., *Journal of Computational Physics* **1997**, *135*.

[6] Dudson B D, Leddy J, *Plasma Phys. Control Fusion* **2017**, *59(5)*.

[7] Ricci P, Halpern F D, Jolliet S, Loizu J, Mosetto A, Fasoli A, Furno I, Theiler C, *Plasma Phys. Control Fusion* **2012**, *54(124047)*.

[8] Tamain P, Bufferand H, Ciraolo G, Colin C, Galassi D, Ghendrih Ph, Schwander F, Serre E, *Journal of Computational Physics* **2016**, *321*.

[9] Oberkampf W J, Roy C J, *Verification and Validation in Scientific Computing*, Cambridge University Press **2010**.

[10] Riva R, Ricci P, Halpern F D, Jolliet S, Loizu J, Mosetto A, *Physics of Plasmas* **2014**, *21*(*062301*).

[11] Dudson B D, Madsen J, Omotani J, Hill P, Easy L, Loiten M, *Physics of Plasmas* **2016**, *23*(*062303*).

[12] Ottaviani M, *Phys. Lett. A* **2011**, *375*(*1677*).

[13] Hariri F, Ottaviani M, *Comput. Phys. Commun* **2013**, *184*(*2419*).

[14] Stegmeir A, Coster D, Maj O, Hallatschek K, Lackner K, *Comput. Phys. Commun* **2016**, *198*(*139*).

[15] Karniadakis G, Israeli M, Orszag J, Hallatschek K, *J. Comput. Phys.* **1991**, *97*(*414*).

[16] Stegmeir A, Coster D, Ross A, Maj O, Lackner K, Poli E, *Plasma Physics and Controlled Fusion* **2017**, *submitted*.

[17] Yu G Q, Krasheninnikov S I, Guzdar P N, *Physics of Plasmas* **2006**, *13*(*042508*).